

PAPER NUMBER

187

CORROSION

April 17-21, 1989

New Orleans Convention Center, New Orleans, Louisiana

89

THE EFFECT OF MICROBIOLOGICALLY INFLUENCED CORROSION ON
STAINLESS STEEL WELDMENTS IN ARTIFICIAL SEAWATER

NICHOLAS J.E. DOWLING, MICHAEL FRANKLIN & DAVID C. WHITE
Institute for Applied Microbiology,
Bldg. 1, Suite 300, 10515 Research Dr.,
Knoxville, TN. 37932.

CHANG H. LEE & CARL LUNDIN.
Dept. of Materials Science and Engineering,
University of Tennessee, TN. 37996.

ABSTRACT

AISI 316L/E308 stainless steel weldments were exposed to unselected marine bacteria over a period of two weeks during which the corrosion rate and parameters influencing that rate were monitored. A model for the microbially influenced corrosion (MIC) of the weldments is proposed using data obtained by Electrochemical Impedance Spectroscopy (EIS), Small Amplitude Cyclic Voltammetry (SACV) and Electron Surface Chemical Analysis (ESCA). Coupons with an as-welded surface condition were shown to corrode fastest in contact with the bacteria.

INTRODUCTION

The corrosion of steels due to microbial attack has long been established fact (1). Recently however, austenitic stainless steels and weldments in particular, were shown to be susceptible to microbiological attack in various environments particularly involving untreated service waters (2,3,4). The possibility that the ferrite/austenite ratio in the welds influenced the MIC process now appears less reasonable (5). The survey of MIC-assisted weld corrosion attack has shown no correlation between the severity of attack and ferrite content. An examination of weld sensitization (intergranular chromium carbide formation and consequent chromium depletion) in the same survey showed that the use of unsensitized material was no protection against MIC attack. These data were obtained however, from welds from different sites where several unknown variables may have exerted disproportionate effect: for example water quality in terms of salinity, pH, suspended particulates,

Publication Right

bacterial content etc. No study (that the authors are aware of) has been carried out under laboratory controlled conditions where the weld thermal history and composition have been correlated with metal loss and bacterial activity of a particular type.

In this article we present data which examines the effect of unselected marine organisms on the corrosion of stainless steel weldments under monitored conditions. The study is used to develop an argument for a corrosion model where localized corrosion is not "evenly" distributed across the surface of weld as might be the case for a coupon of uniform composition and no residual stresses eg. unwelded 316L. The model assumes that "localized" corrosion occurs at certain sites only as dictated by the prior thermal history, galvanic effects of introducing a filler metal of slightly different composition and microbial activity. Abiotic corrosion tests with the same welds are an important part of the data required to develop the model.

MATERIALS AND METHODS

All coupons were of dimensions 2 x 2 x 0.3 cm and made of AISI 316L stainless steel (low carbon) nuclear grade base metal (C 0.016%, Mn 1.66%, P 0.024%, S 0.011%, Si 0.47%, Cr 16.3%, Ni 10.13%, Cu 0.18%, Mo 2.11%, Co 0.2%, N 0.05%). The coupons included autogenous welds, in both 600 grit finished and as-welded conditions, and welds made with E308 filler metal, also in the polished and as-welded condition. 600 grit surface finished base metal coupons of unwelded 316L were also exposed. The ferrite content of the autogenous and filler metal added welds were 3.8 and 5.5 FN respectively measured by Magne-Gage.

The coupons used a soldered connection to a copper wire on the obverse surface to that exposed and were mounted in epoxy. In order to remove the possibility of edge crevice corrosion in both biotic and abiotic experiments the procedure after Lee et al. (6) was employed. Polished samples were prepassivated with 50% nitric acid and the edges painted with an epoxy sealant (Armstrong products, Warsaw, IN.). The prepassivated surfaces remaining exposed were then polished to a 9 u diamond finish, degreased with acetone and exposed. The as-welded coupons were simply mounted in epoxy and sealed as above. The coupons were exposed in the pipe container with three replicates for each condition.

Prepared coupons were placed in the bottom of 6 inch diameter, 3 feet long polypropylene pipes with the coupon surfaces flush with the interior of the pipe (see figure 1). Arrangements were made to provide a conventional three electrode cell for each coupon including a salt bridge to a saturated calomel electrode (SCE) and a titanium counter electrode with at least four times the surface area of the working electrode (coupon under test).

Sterilization of the pipes was with 4% formaldehyde for 1 hour after which the pipe was sequentially rinsed with 2 litres of sterile distilled water. To ensure sterility the sterile pipes were supplemented with 5 mM sodium azide.

The medium contained the following (g/L distilled water): microcrystalline cellulose 2, cellobiose 1, chitin 0.125, yeast extract 0.1, starch 0.5, "Instant Ocean" (Aquarium systems, Ohio) 30, complex vitamins (7) and trace elements (8) On

cooling the medium was adjusted to pH 7.5 and 16 litres were pumped into each pipe via an end port.

The pipes were inoculated with 10 mls of identical medium to that above that had previously been inoculated with black sulphide-rich marine sediment.

Abiotic experiments involved suspension of mounted coupons in glass vessels (operating liquid volume 850 mls) also in a similar three electrode arrangement. The glass vessels were gas-tight and equipped with sparging stones. Several corrosive electrolytes were employed including 1N H₂SO₄, 3% NaCl with varied concentrations of organic acids, and FeCl₃.

Electrochemical techniques used included electrochemical impedance spectroscopy (EIS), small amplitude cyclic voltammetry (SACV), and cyclic anodic polarization (CAP) sweeps. EIS analysis was between 10 KHz and 3 mHz with an average value taken over 5 cycles of amplitude 5 mV rms. All measurements were taken at the open circuit potential. EIS data was presented in three formats: 1) Complex plane (Nyquist) plot where Z' (real impedance) is ordinate to the -jZ'' (imaginary impedance). Frequency is implicit. The total impedance Z is related:

$$Z = Z' + jZ'' \quad (j = -1)$$

2) Bode plot where total impedance Z is plotted versus the angular frequency (ω), and 3) Phase angle plot where the phase shift is noted with respect to the frequency (ω).

SACV analysis was performed as galvanostatic oscillations around zero current with maximum amplitude 1 μ A. The sweep rate was approximately 0.2 mV/sec. CAP sweeps were carried out at 0.167 mV/sec rate from E_{corr}. (the open circuit potential) to 1.2 V/SCE.

Electrochemical measurements were all related to the Stearn-Geary equation:

$$I_{corr} = \frac{ba \cdot bc}{2.303 (ba + bc) R_p}$$

where I_{corr} is the corrosion rate in amperes/cm², ba and bc are the anodic and cathodic Tafel parameters respectively, and R_p is the polarization resistance. Thus R_p is inversely related to the corrosion rate.

Electron surface chemical analysis (ESCA) was carried out using a Perkin Elmer PHI 5100 with a hemispherical capacitor analyser parameters: 250 watts X-ray flux, pass energy = 89.5 V. Sputtering was up to 30 mins with an Argon ion beam set to 4 kV.

Total cell counts were obtained using a Petroff-Hauser counting chamber to establish the number of cells/ml. Organic acid analysis was with a Shimadzu GC-9A gas chromatograph equipped with SP-1220 packing (Supleco, Bellafonte, PA.).

RESULTS

Two series of tests were carried out in the presence of microorganisms: the first involving a comparison of the corrosion rates and impedance spectra of autogenous welds on 316L base metal (polished without surface welding oxides) and as-welded (with the welding oxides intact) and polished 316L base metal. The second test compared the effect of surface treatment on E308 filler metal added in the as-welded and polished conditions. After inoculation the autogenous weld and base metal coupons were examined every day for open circuit potential (OCP) movement and every two days for polarization resistance values by SACV and EIS. Total exposure time was 2 weeks.

Within three days the OCP for all inoculated coupons had moved into the active region (approx. -0.46 V/SCE) with respect to the sterile coupons (approx. -0.03 V/SCE, figure 2) while the value for R_p (polarization resistance) decreased for the autogenous-welded and unwelded inoculated coupons to about 2 kOhms.cm⁻². Correspondingly the values for the sterile coupons were in the region of 20 kOhms.cm⁻² (9).

SACV data for the welds using E308 filler metal is presented in figure 3. EIS data is also presented for the autogenous (figure 4) and E308 welds (figures 5 and 6) in the corrosion test electrolytes (inoculated vs. sterile marine medium).

ESCA results are presented in figures 7 and 8 where the element profiles of the weld-related oxides in the heat affected zones of the as-welded and polished welded conditions are compared.

The results of abiotic analyses of the weldments are also presented. Figure 9 clearly shows the two time constants involved in the corrosion of a polished 316L/E308 weld in deaerated 1N H₂SO₄. Further development is observed when increasing quantities of chloride (as sodium salt) are added (figure 10). Finally the effect of deaerated FeCl₃ on a polished 316L/E308 weld is shown in figure 11.

Bacterial numbers in the inoculated pipes attained approximately 1E9/ml while no cells were observed in the sterile pipes. Acetic and butyric acid were produced by the bacteria to about 4 mM each. This lowered the pH to around 4.5.

DISCUSSION

(i) Autogenous weldments and base metal corrosion

Stainless steels possess "superior" passive films composed mainly of chromium and nickel with bound water (10). The corrosion model of stainless steels therefore involves the dynamics of local penetration of these films and their repassivation which determines the overall rate of metal loss (11). In the 300 series stainless steels molybdenum is added (approximately 2% for AISI 316) to stabilize the pitting susceptibility with the MoO₄⁻² anion (12). Welding processes however appear to disturb the passive film at the fusion line and promote localized corrosion by

solidification and segregation in autogenous welds of 316L and 317L in acid oxidizing environments (13) resulting in corrosion of interdendritic austenite. On the other hand wrought duplex alloys in reducing acids showed preferential attack in the delta-ferrite (14,15). Thus both phases of duplex stainless steels may be preferentially attacked although under different conditions.

Bacteria apparently attack both phases (5) although in oxygenated seawater little preferential attack was observed in autogenous welds (16) and correspondingly little significant increase in crevice attack. In our study the effect of autogenous welding on 316L showed that in stagnant conditions the average corrosion rate in as-welded surfaces was significantly less than that observed with 600 grit surface welds or unwelded 316L base metal (9). In order to promote the propagation of pitting attack in stainless steels the oxygen content must be removed to low levels. The microbiological media used in this study was designed to mimic estuarine seawater where suspended particles act as a support matrix for the bacteria and contribute to the biofilm and associated diffusion processes. For example precipitated cellulose fragments increase the oxygen diffusion boundary.

The onset of microbiological attack was marked by the movement of the open circuit potential into the active region (approximately -0.4 V/SCE). This was taken to indicate the commencement of pitting and removal of oxygen local to the metal surface. Average values for the polarization resistance (R_p) obtained by SACV and EIS indicated that the autogenous as-welded coupons corroded slower than either the polished welds or 316L base metal. EIS data (figure 4) showed that two relaxations were involved in the corrosion processes associated with the polished coupons over the frequencies examined. The corresponding EIS data for the autogenous as-welded coupons showed the high frequency end of a single depressed capacitive loop. This difference was ascribed to surface heat-tinting (mostly oxides of chromium) obscuring the surface. Conversely Kearns (17) showed that autogenous welds with high alloyed stainless steels showed significant preferential attack at the heat affected zones (HAZ) where chromium oxide tinting was at a maximum.

(ii) Corrosion of weldments with E308 filler metal.

In the second part of the study, welds incorporating filler metal (E308) were examined in a similar pipe system as above but quite different results were obtained. Values obtained for R_p by SACV (figure 3) show that the average corrosion rate was fastest for the as-welded inoculated state. After a two week exposure the 316L/E308 welds in contact with the bacteria were covered with a red deposit in the HAZ only. In contrast the weldments exposed to sterile marine conditions had no such red deposit. No observable affect was manifest in the polished welds although the SACV measurements demonstrated a significant increase in corrosion rate with the presence of bacteria. Clearly surface polishing had a significant effect on the corrosion rate. EIS data (figure 5 & 6) also demonstrate that surface polishing had a improved effect on the overall corrosion mechanism: examination of the phase angle with respect to frequency (figure 6) shows that there are two distinct relaxations involved in the corrosion process in the as-welded inoculated state. All other conditions were characterized by a single relaxation in the frequencies examined. Figure 5 is a Bode plot which demonstrates the variation of impedance Z with frequency and has the virtue of presenting the impedance for all the frequencies in

discrete form. The as-welded inoculated state is characterized by a step at approximately 2 Hz which corresponds to the sum of R_p and the uncompensated resistance, thus it is seen that the as-welded inoculated state has the fastest corrosion rate. This data was corroborated by SACV.

The as-welded coupons are clearly more susceptible to MIC than other coupon surface types (figure 3). Borenstein (in this symposium) has presented data which shows that the as-welded state in "fresh water" systems (ie relatively low chloride content) is more susceptible to MIC attack than corresponding solution-annealed or nitric acid passivated welds. Thus demonstrating that surface conditioning of weldments is critical to the initial MIC pitting response. The autogenous weld EIS data (figure 4), however, showed that not only was the corrosion rate slower with the as-welded state but the mechanism was different. The polished autogenous welds behaved very similarly to polished unwelded 316L base metal. Thus it appears that the nature of the filler metal (perhaps a galvanic couple) seriously changes the corrosion characteristics.

Post-exposure examination of the weld-induced oxides using element profiling with ESCA showed that the as-welded filled weldments apparently had iron and chromium closer to the surface in the presence of the bacteria than the sterile system. The as-welded oxides (figure 8) were clearly thicker and more diverse than on the polished welds (figure 7) which had very uniform composition throughout their thickness below the surface (10 mins sputtering time with the Argon beam). Chloride anions were shown to penetrate far into the oxide layer which would tend to follow the "Point defect model" proposed by MacDonald and coworkers. Interestingly a strong nitrogen presence was shown at the surface of all of the oxides in contact with the bacteria which may be attributed to proteins associated with the bacteria. Chamberlain and Garner (18) have noted similar nitrogen rich surfaces on marine-exposed copper/nickel alloys which they attributed to marine microbiota.

Abiotic experiments were carried out on all the materials exposed to the bacteria which consisted of manipulating the electrolyte (i) in order to mimic the corrosion mechanism and rates associated with the presence of the bacteria, and (ii) to examine the corrosion characteristics of weldments and base metal in contact with standard corrosive electrolytes. The corrosion rates of 316L/E308 weldments in contact with 3% NaCl, 4 mM acetic acid, 4 mM butyric acid, and pH=4.5 while sparging with nitrogen, were significantly slower than those obtained with bacteria. Thus it appears that other mechanisms are involved or a greater magnitude of the processes currently considered to be likely modes of MIC attack. For example anion concentration by the bacteria (high chloride) combined with low local pH which may be as low as 2.0 unlike the bulk pH which was 4.5.

Experiments were also performed to determine the impedance behaviour of the materials under "ideal" environments in order to interpret the diagrams obtained in bacterial exposure experiments. The results of a 316L/E308 weld in sulphuric acid (1N) deaerated with nitrogen gas is conveniently displayed in a complex plane plot (figure 9) and had two relaxations. The first (high frequency relaxation) was interpreted in terms of a parallel circuit associated with the double layer capacitance and charge transfer resistance. The second (low frequency relaxation) was interpreted in terms of a diffusion process associated with pit solution

impedance after De Levie (19) who used a "transmission" line model to account for identical non-interconnected pores on an electrode surface. Oltra and Keddam (20) have developed this model and described localized corrosion in terms of pits being small conducting disks in insulating planes at low frequencies. At high frequencies, however, the whole electrode surface behaves as a conductor.

Introduction of chloride ions into the sulphuric acid to promote pitting (figure 10) tended to reduce the contribution of the low frequency loop. Exposure to Ferric Chloride however, removed the low frequency loop altogether (figure 11), which implies that most of the faradaic current originates from the pits in chloride-rich environments. Subsequent anodic polarizations in Ferric Chloride showed the selective removal of the austenitic phase in the weld metal and grain dropout in the HAZ which in some cases has been the case in environmental failures.

In a mathematical model for this case the pores of De Levie (19) take the form of pits in the surface oxide crystal lattice. The corrosion reactions with bacterial medium are complicated by diffusion constraints: it is quite clear that bacteria promote corrosion and other electrochemical reactions while strongly adhered to available surfaces (21) and there introduce diffusion gradients.

How then can the stainless steel coupons be affected by the bacteria? Hakkarainen (22) showed that the internal electrode potential of propagating pits was much lower than that potential measured from the bulk solution. Thus in a low pH, high chloride environment where the redox potential is artificially lowered (such as colonized surfaces in natural seawater) repassivation is a less likely event. Bacteria collude to remove oxygen and excrete reduced products which collectively lower the redox potential. If a pitting process has initiated then such conditions would tend to encourage propagation. The model suggested for the corrosion of AISI 316L/E308 welds by bacteria in a high chloride level environment allows increased dissolution of iron from the HAZ as a direct result of the depletion of the chromium content from the underlying metal below the welding oxide films (figure 12). The ferric chloride attack shows that pit nucleation occurs at the fusion line and the pits propagate into the HAZ. The HAZ is the same region where most of the metal loss occurs when in contact with the bacteria. If the corrosion processes in Ferric Chloride attack are similar to bacteria corrosion then it might be expected that the bacteria would selectively attack the austenite phase in under these conditions.

While the reasons for the application of EIS to MIC-related problems are many (less disturbance of biofilms, mechanistic information etc), the isolation of independent processes involved in the corrosion of stainless steels in terms of impedance data has progressed very little. The corrosion of stainless steels is very complex and not well understood. The introduction of specific bacteria, however, with known capabilities will provide "new" ways to perturb the corrosion behaviour of these alloys and perhaps provide new insight into their corrosion processes.

CONCLUSIONS

- 1) Bacteria in the marine environment may significantly accelerate selective corrosion of the heat affected zone of a weld.

2) The establishment of a biofilm at the surface of the metal using a relatively inert matrix (fragmented cellulose) appears to increase the corrosion rate (probably a significant effect is the prevention of oxygen reaching the surface and the consequent prevention of the repassivation of the metal surface).

3) The introduction of stainless steel coupons into sterile chloride-rich, low pH (4.5), deaerated electrolyte containing volatile fatty acids in similar concentrations to that produced by the bacteria, produced a much lower corrosion rate than that demonstrated by the bacteria. Therefore some effect produced by the bacteria is not being considered.

4) The corrosion processes of 316L base metal in contact with bacteria appears to have two relaxations the lower frequencies of which may be involved in the impedance associated with pits.

5) Preferential attack of both autogenous and filler metal added welds appears to be dictated by the surface condition, at least in the initial stages. The rate of corrosion was fastest in 316L/E308 weldments with an as-welded surface. EIS data showed that the corrosion was again characterized by two relaxations.

6) Abiotic experiments with 316L base metal, 316L autogenous welds, and 316L/E308 welds showed that pitting attack only occurred in specific conditions. Ferric Chloride with selective removal of austenite severely pitted the HAZ (with anodic polarization) and demonstrated a single relaxation. Deaerated H₂SO₄ however, produced two distinct relaxations and etched the weld metal in a distinctive manner.

7) It is commonly believed that bacterial attack behaves similarly to the action of Ferric Chloride on austenitic stainless steels. In this experiment the bacteria appeared to remove metal in the HAZ of the 316L/E308 weldments while the weld metal itself was less attacked. This was very like the action observed with both 1% and 10% Ferric Chloride.

ACKNOWLEDGMENTS

The authors would like to thank David Harkins for very kindly performing the ESCA analyses. The US Navy is thanked for providing funds via the Office of Naval Research grant numbers: N00014-86-K-0275 and N0014-87-K-0012. David Ringleberg is thanked for the excellent diagrams.

LITERATURE CITED

1. H.H. Uhlig. The Corrosion Handbook. J.Wiley & Sons, New York. 1948.
2. R.E. Tatnall. Case Histories: Bacteria Induced Corrosion. Corrosion 19(8), 41-48.1981

3. G. Kobrin. Corrosion by Microbiological Organisms in Natural Waters. Corrosion 15(7), 38-43. 1976.
4. S.W. Borenstein, and P.B. Lindsay. Microbiologically influenced corrosion failure analyses. Materials Performance 27, 51-54. (1988)
5. S.W. Borenstein. Microbiologically influenced corrosion failures of austenitic stainless steel welds. Corrosion/88. Paper No.78. National Association of Corrosion Engineers, Houston, Texas 1988.
6. I.-S. Lee, E.E. Stansbury, and S.J. Pawel. The determination of pitting susceptibility with a new sample preparation technique. Corrosion. Accepted for publication August 1988.
7. N.J.E. Dowling, P.D. Nichols, and D.C. White. Characterization of a sulphate-reducing consortium with phospholipid fatty acids and infra-red spectroscopy. FEMS Microbial Ecol. Accepted for publication. 1988
8. N. Pfennig, F. Widdel, and H.G. Truper. The dissimilatory sulphate-reducing bacteria. In: The Prokaryotes. Vol.1, pp926-940. Eds. Starr, M.P., Stolp, H., Truper, H.G., Balows, A., and Schlegel, H.G. Springer-Verlag, Berlin & New York. 1981
9. N.J.E. Dowling, C. Lundin, C.H. Lee, M. Franklin, and D.C. White, Enhanced corrosion rates of 316 AISI weldments in the marine environment due to bacteria. The 7th International symposium for marine corrosion and fouling. 7-11th Nov., Valencia, Spain. 1988
10. G. Okamoto. Passive film of 18-8 stainless steel structure and its function. Corrosion Science. 13, 471-489. 1973
11. L.F. Lin, Y.Y. Chao, and D.D. MacDonald. A point defect model for anodic passive films. II. Chemical breakdown and pit initiation. J. Electrochem. Soc. 128, 1195. 1981
12. P. Vanslambrouck, W. Bogaerts, and A. Van Haute. The role of molybdenum in the inhibition of passivity breakdown in neutral chloride solutions up to 2500C. Passivity of metals and semiconductors. Proceedings of the 5th International symposium on Passivity, Bombannes, France. 30th May-3rd June, 1983. Elsevier, Amsterdam. 1983
13. A. Garner. The effect of autogenous welding on chloride pitting corrosion in austenitic stainless steels. Corrosion 35(3), 108-113. 1979
14. Y.-H. Yau and M.A. Streicher. Galvanic corrosion of Duplex FeCr-10% Ni Alloys in reducing acids. Corrosion 43(6), 366-373. 1987.
15. P.E. Manning, D.J. Duquette, and W.F. Savage. The effect of test method and surface condition on pitting potential of single and duplex phase

304L stainless steel. Corrosion. 35, 151-157. 1979

16. A. Garner. Crevice corrosion of stainless steels in seawater: Correlation of Field data with laboratory ferric chloride tests. Corrosion 37(3), 178-184. 1981
17. J.R. Kearns. The corrosion of heat tinted austenitic stainless alloys. Corrosion-85. Paper No.50. National Association of Corrosion Engineers, Houston, Texas. 1985
18. A.H.L. Chamberlain and B.J. Garner. The influence of iron content on the biofouling resistance of 90/10 Copper-Nickel alloys. Biofouling 1, 79-96. 1988
19. R. De Levie. Electrochemical response of porous and rough electrodes. In: Advances in Electrochemistry and Electrochemical Engineering. Vol.6, 329-397. 1969
20. R. Oltra and M. Keddam. Application of impedance technique to localized corrosion. Corrosion Science 28 (1), 1-18. 1988
21. M. Mittleman and G.G. Geesey. Biological Fouling of Industrial water systems. A problem solving approach. Water Micro Associates, PO Box 28848, San Diego, CA 92128-0848. 1987
22. T. Hakkarainen. Repassivation potential of corrosion pits in stainless steel. In: Passivity of Metals and Semiconductors. Elsevier, Amsterdam, New York. 1983

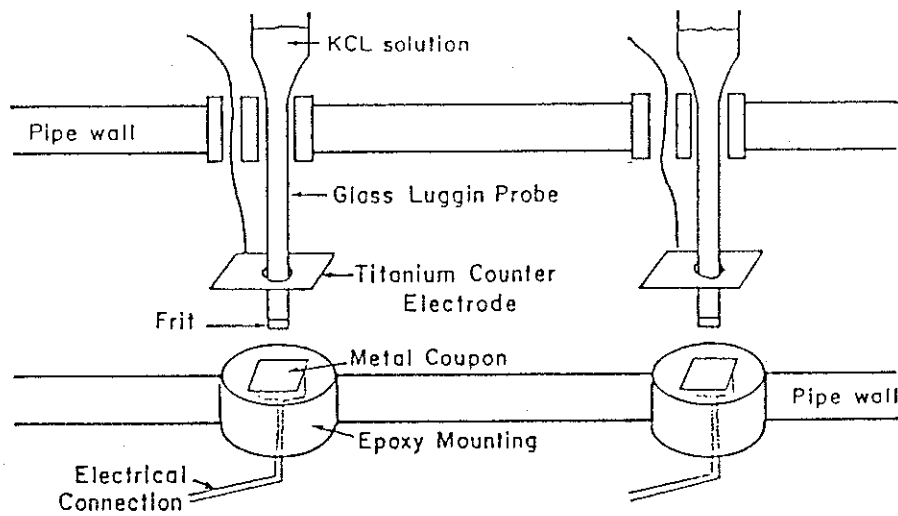


Figure 1: Electrode arrangement of the test system

Open-Cell Potential of Coupons Over Two Weeks

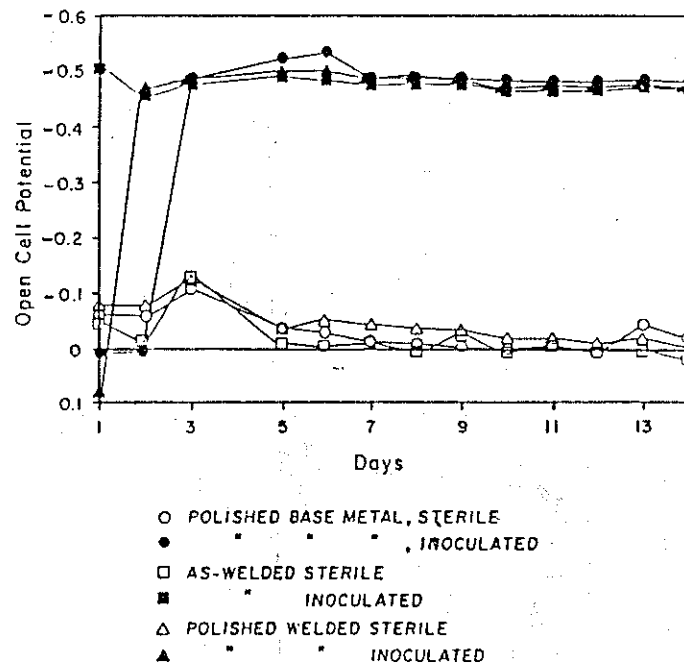


Figure 2: Evolution of the open-circuit potential with time of autogenous welds and base metal.

Evolution of Polarization Resistance (R_p)
for Polished Welded (PWF) and As-Welded (AWF)
316L Coupons with E308 Filler Material

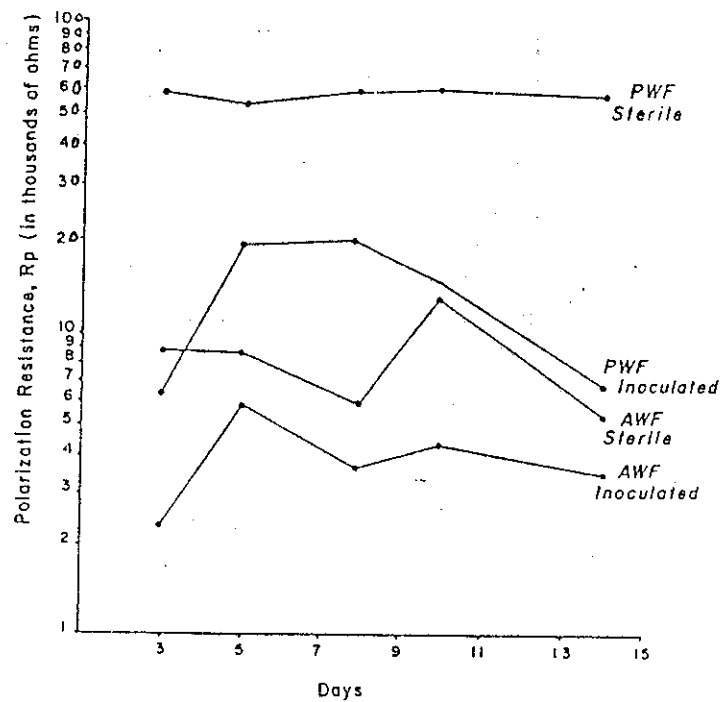


Figure 3

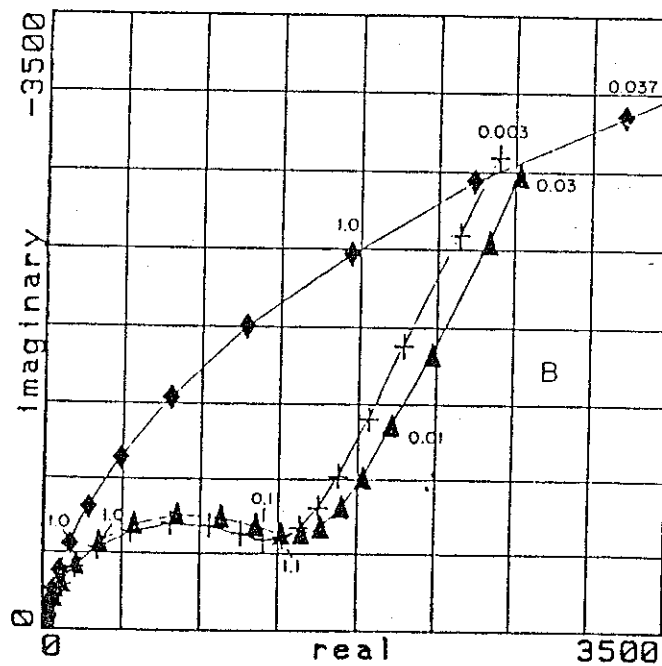


Figure 4: Electrochemical impedance data showing the effect of marine bacteria on polished 316L base metal (cross), polished autogenous weld (triangle), and autogenous as-welded condition (diamond).

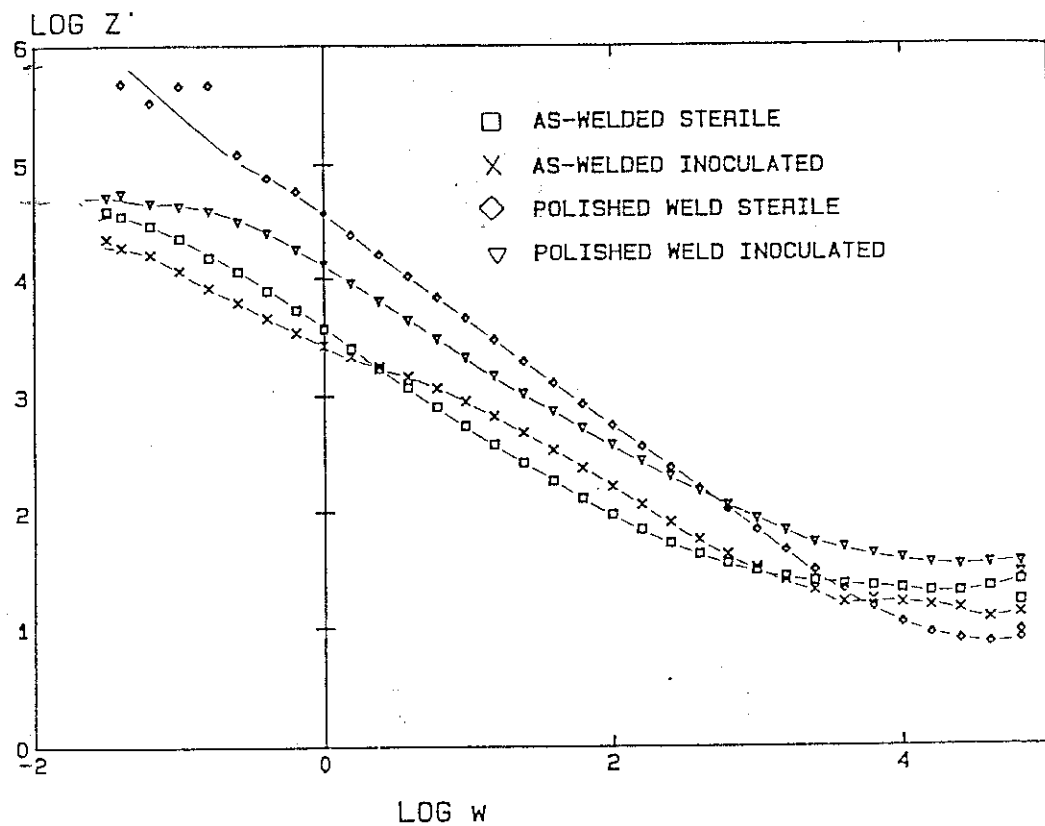


Figure 5: Electrochemical impedance data showing the distribution of impedance with frequency (Bode plot) for the polished and as-welded conditions of 316L/E308 welds.

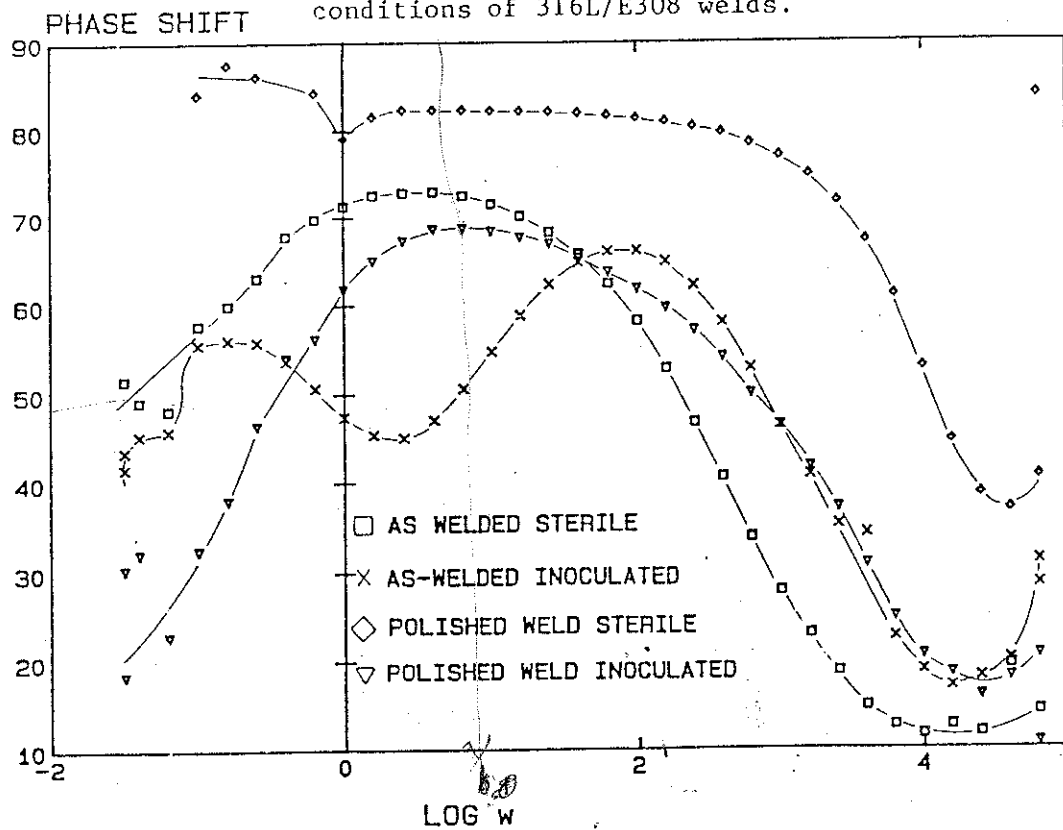


Figure 6: Electrochemical impedance data as for figure 5 however presented to show the two relaxations associated with the as-welded state.

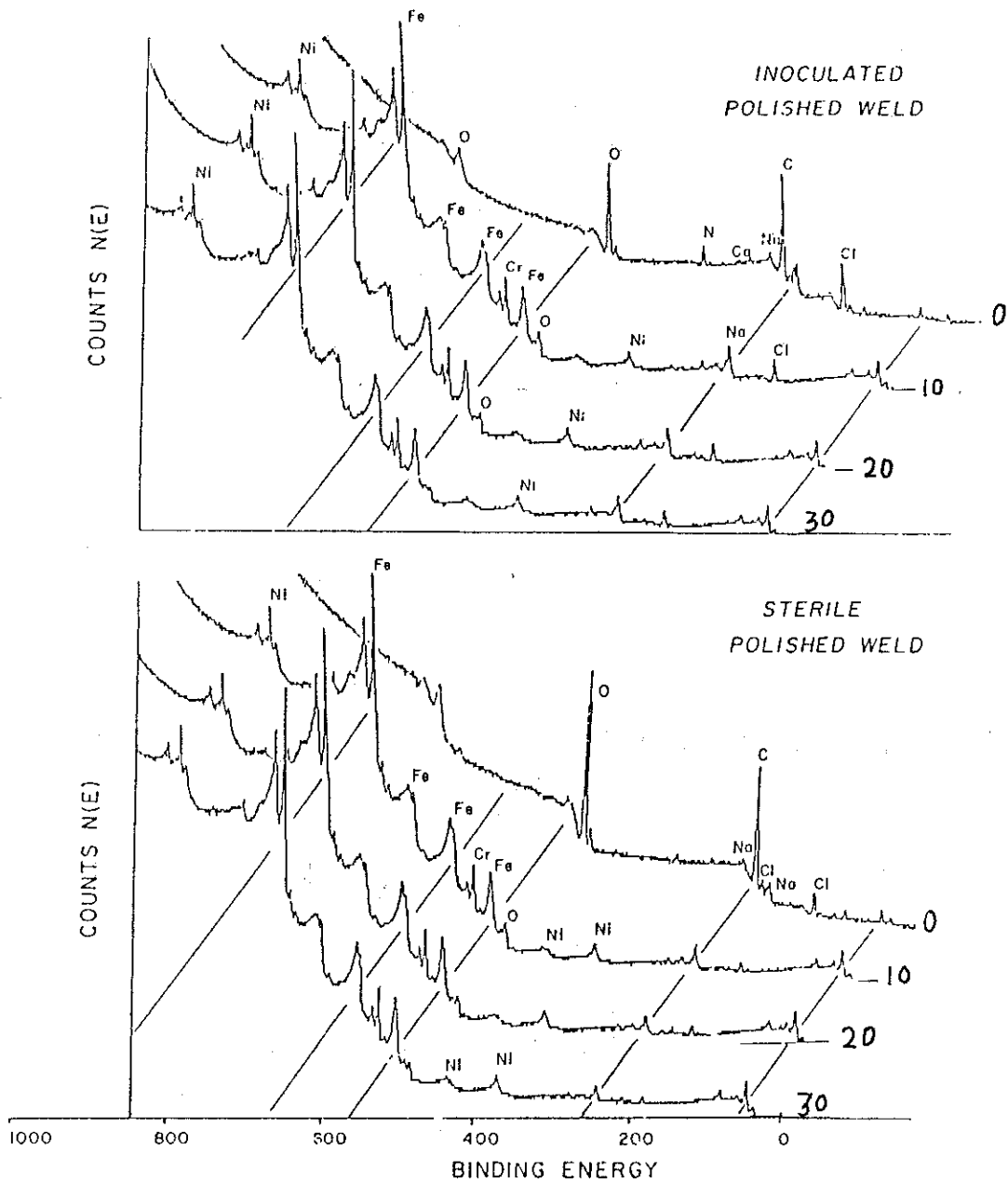


Figure 7: ESCA analyses of the polished welds exposed to bacteria and sterile conditions respectively.

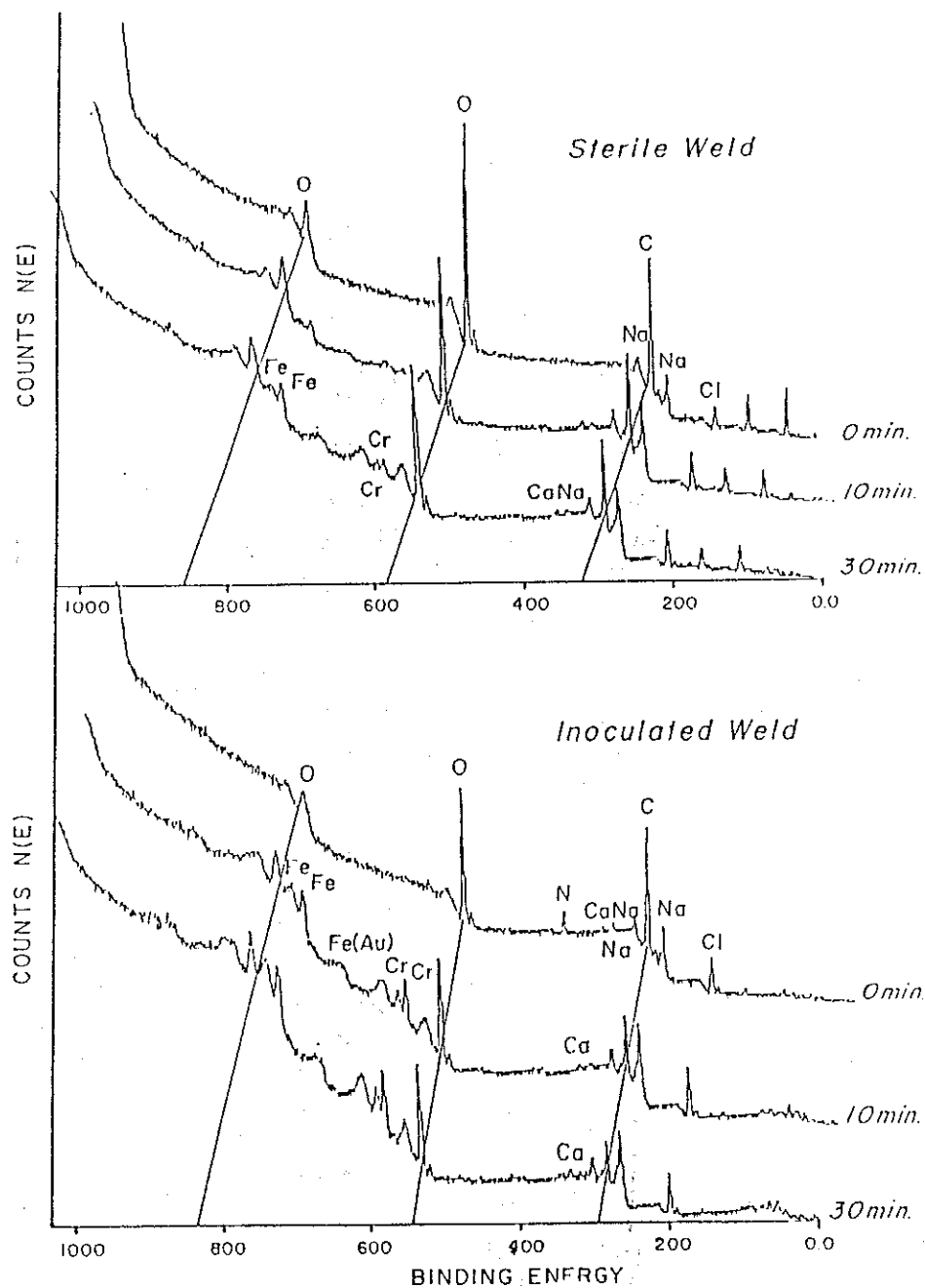


Figure 8: ESCA analyses of the as-welded 316L/E308 coupons after exposure to sterile and inoculated test conditions respectively.

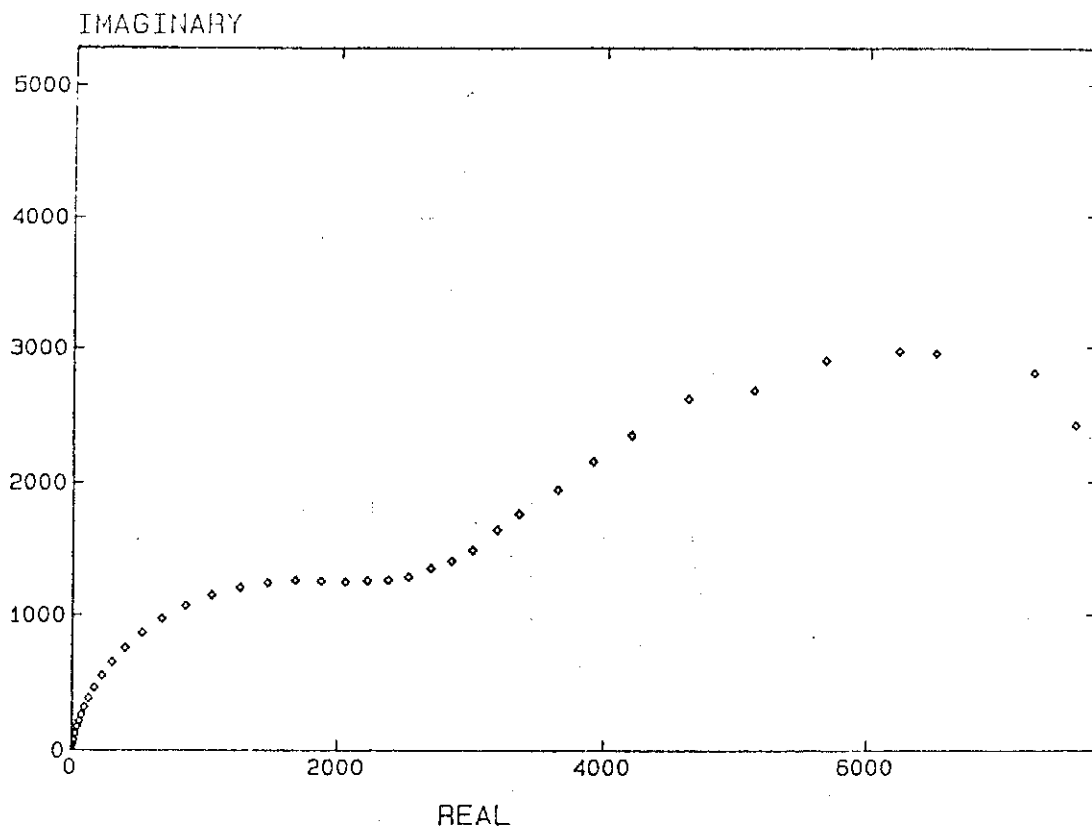


Figure 9: Electrochemical impedance data of a 316L/E308 weld exposed deaerated 1N H₂SO₄ demonstrating two relaxations.

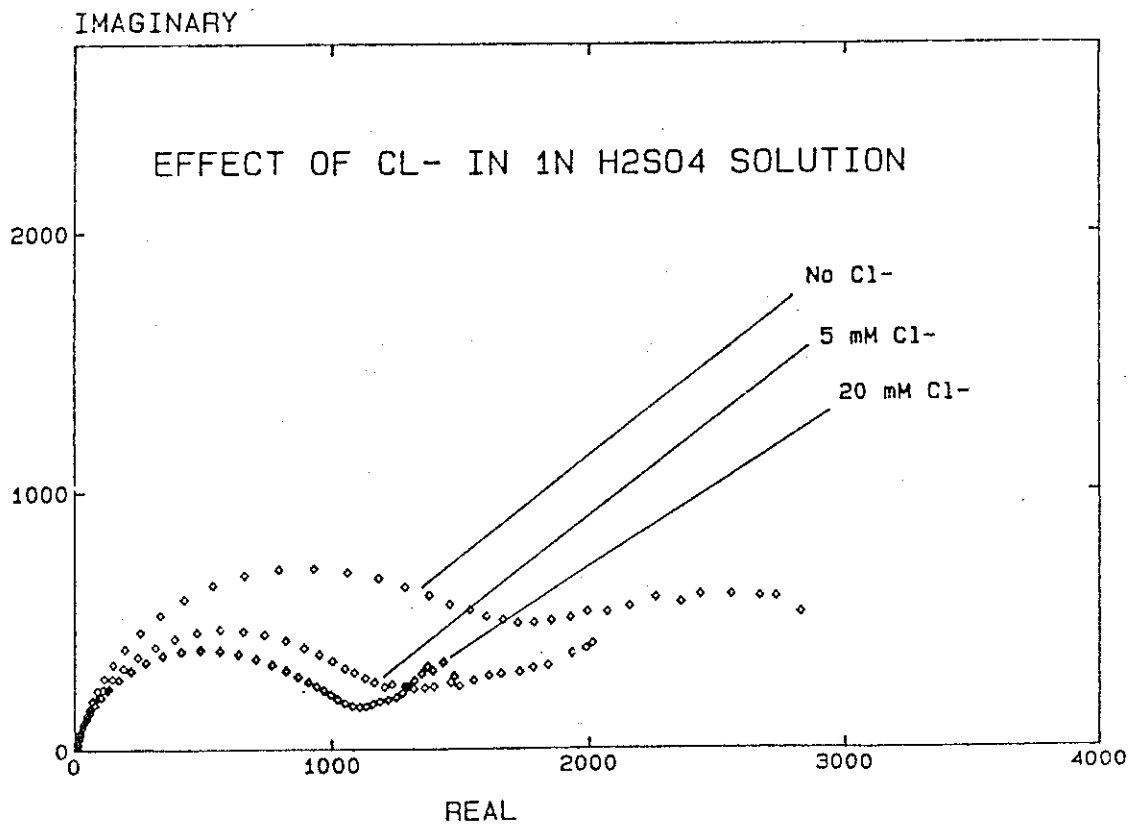


Figure 10: Electrochemical impedance data showing the effect on 316L/E308 welds of adding chloride to 1N H₂SO₄.

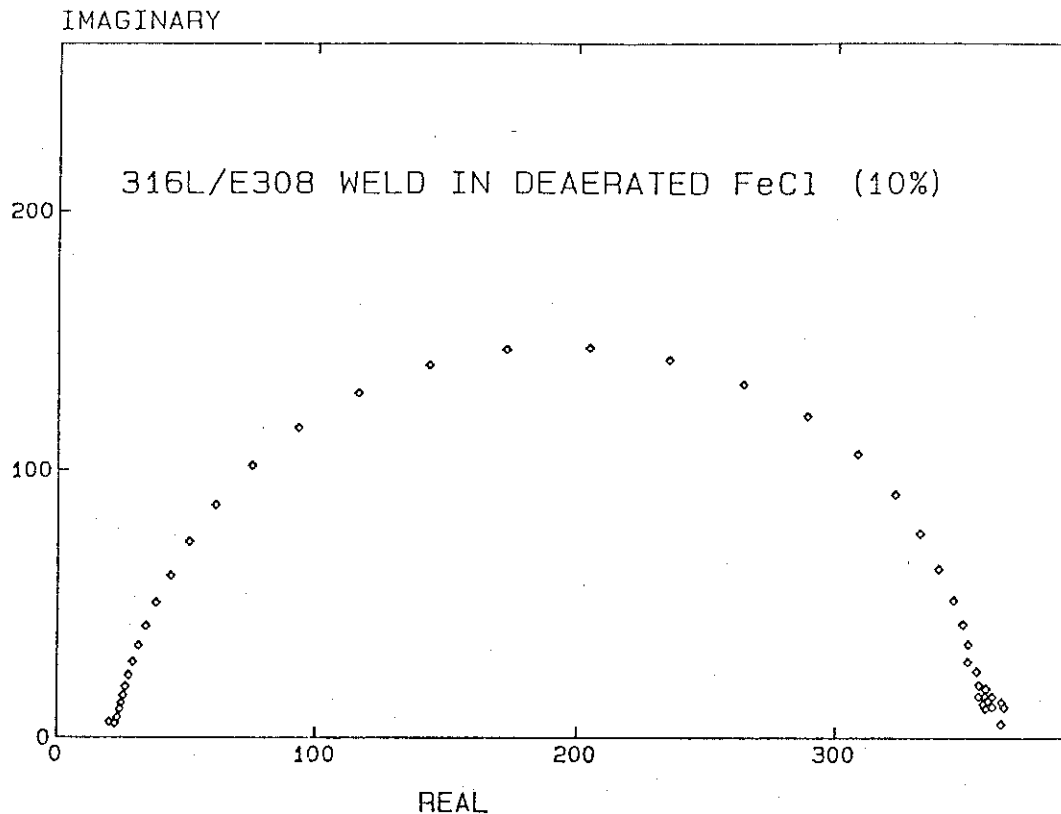
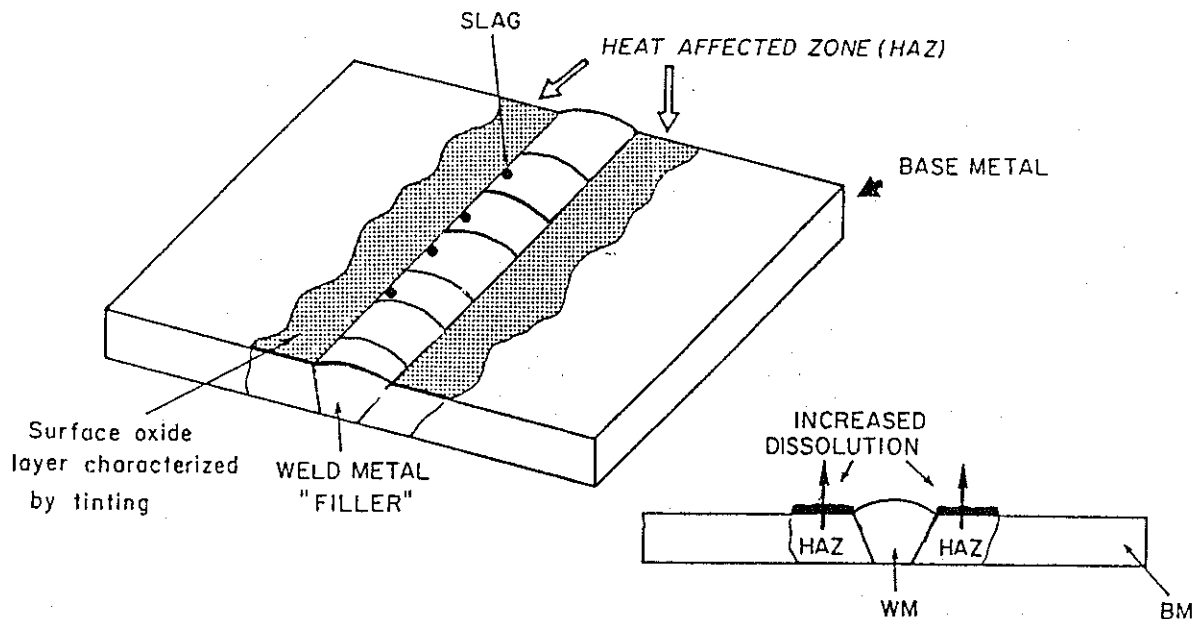


Figure 11: Electrochemical data showing the effect of Ferric Chloride on 316/E308 weldment.



During the welding process chromium is depleted in the HAZ and hence the metal underlying the Cr^{+3} rich surface is more susceptible to dissolution.

Figure 12: Suggested model for corrosion of a 316L/E308 weldment in contact with marine bacteria.